The bone and cartilage interplay in osteoarthritis: key to effective treatment strategy

Tuerlings, M.

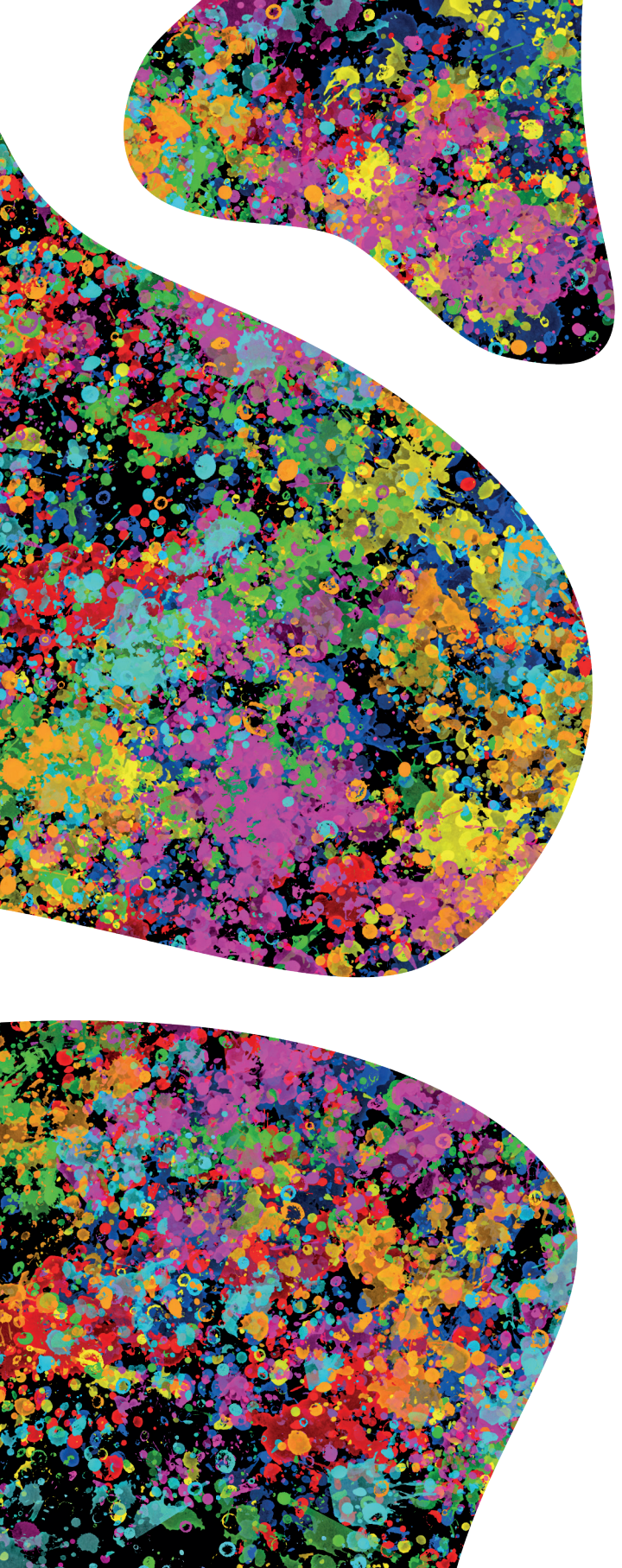

CHAPTER 5

Characterization of underlying subchondral bone of identified OA molecular endotypes in articular cartilage

Margo Tuerlings[1], Ilja Boone[1], H. Eka D. Suchiman[1], Nico Lakenberg[1], Robert J.P. van der Wal[2], Rob G.H.H. Nelissen[2], Yolande F.M. Ramos[1], Rodrigo Coutinho de Almeida[1], Ingrid Meulenbelt[1]

[1] Dept. of Biomedical Data Sciences, Leiden University Medical Center, Leiden, The Netherlands.
[2] Dept. Orthopaedics Leiden University Medical Center, Leiden, The Netherlands.

Abstract

Objective: To characterize the underlying subchondral bone transcriptomic profile of previously identified OA molecular endotypes in OA articular cartilage.

Methods: Previously generated mRNA-seq datasets of articular cartilage (N=56 patients) and subchondral bone (N=24 patients) were combined (N=14 patients of whom both articular cartilage and subchondral bone mRNA-seq data were available) to characterize the underlying subchondral bone of molecular endotype A and B previously identified in articular cartilage. Differential expression analysis between subchondral bone of endotype A and B patients was performed. Moreover, differential expression analysis between preserved and lesioned OA subchondral bone stratified for OA molecular endotype was performed. Generalized estimating equations (GEE) was applied to find association between genes that mark OA endotype in bone and radiographic phenotype joint space narrowing (JSN) scores.

Results: Upon comparing gene expression levels of the underlying subchondral bone between OA molecular endotype A and B, we found 543 genes being FDR significantly differentially expressed. Similar to articular cartilage, these 543 differentially expressed genes in subchondral bone were enriched for processes such as immune response (GO:0006955), characterized by expression of *IL1B* (FD=3.98, FDR=4.11x10^{-3}), *TNFSF14* (FD=7.48, FDR=1.44x10^{-2}), and *OSM* (FD=6.31 FDR=1.19x10^{-4}), with higher expression of these genes in molecular endotype B compared to A. Upon calculating association beteween gene expression levels and radiographic phenotypes, we found *RSP7P1* and *NSA2* being positively associated to JSN and these genes were higher expressed in endotype B compared to endotype A patients. On the other hand, we found *ZFP41* and *NOTCH4* being negatively associated to JSN and these genes showed higher expression in endotype A compared to endotype B patients. The latter confirms the association between endotype B and increased JSN, which is also observed in articular cartilage.

Conclusion: Altogether, we here showed that underlying bone of OA endotypes identified in articular cartilage is significantly different between OA molecular endotypes. We showed that OA endotype B was associated with excessive bone formation, in line with increased joint space narrowing. Moreover, OA endotype A was associated with increased expression of neuronal markers, suggesting these patients might experience pain in an earlier OA stage compared to endotype B OA patients.

Introduction

Osteoarthritis (OA) is a highly prevalent heterogeneous disease of the whole joint, characterized by, amongst others, articular cartilage degeneration and subchondral bone remodeling [1, 2]. OA has a considerable genetic component and previous comprehensive genome wide association studies (GWAS) have identified OA risk genes, such as *WNT10B, TNFSF11,* and *IL11,* that are involved in maintenance processes in both articular cartilage and subchondral bone, indicating that both tissues are involved in initiation and progression of OA pathophysiology [3-7]. Prevalence of OA is increased among elderly and pain and stiffness are hallmark symptoms of OA. As such, OA is known to cause substantial effects on quality of life. Yet, no treatment options are available to prevent, slow down, or cure OA, except for total joint replacement surgery at end-stage OA [8]. Failure in development of OA disease modifying treatments might be due to OA heterogeneity, that does not accommodate the one-drug-fits-all-patients design applied thus far [9]. In this respect, Soul et al [10] reported on the identification of two OA molecular endotypes using RNA-sequencing (RNA-seq) of articular cartilage, which we confirmed in an independent dataset [11]. The two identified endotypes represented chondrocyte hypertrophy pathway and immune response pathway, respectively. Moreover, we showed that joint space width was significantly lower (increased joint space narrowing (JSN)) in endotype B compared to endotype A patients [11]. Subsequently, to make these OA molecular endotypes more applicable to clinical practice, we focused on identification of circulating miRNAs that can be used to stratify patients into OA endotype before a potential treatment strategy starts (**Chapter 4**). Moreover, we proposed potential therapeutic targets for both endotypes by combining differential expression analysis data with GWAS and allelic imbalance data. As such, we identified *MAP2K6* as potential druggable target for endotype A patients and *HLA-DPA1* as potential druggable target for endotype B patients. Although effort has been made to identify and characterize these OA endotypes in articular cartilage and find biomarkers in blood plasma, the underlying subchondral bone remains unexplored. This despite the fact that subchondral bone contributes to onset and progression of OA as shown by genetic studies [7], indicating that these differences, and hence optimal treatment options, can also originate from subchondral bone. Therefore, in the current study we set out to characterize OA molecular cartilage endotypes in the underlying subchondral bone by using our previously described RNA-seq datasets [12, 13].

Methods

Sample description

This study includes 66 patient of the RAAK study, who underwent a joint replacement surgery due to OA. Macroscopically preserved and lesioned OA articular cartilage and its underlying subchondral bone were collected as described previously [14]. Informed consent was obtained from all participants and ethical approval for the RAAK study was given by the medical ethics committee of the Leiden University Medical Center (P08.239/P19.013).

mRNA sequencing

Total RNA was isolated from articular cartilage and subchondral bone using Qiagen RNeasy Mini Kit (Qiagen, GmbH, Hilden, Germany). Paired-end 2×100 bp RNA-sequencing (Illumina TruSeq RNA Library Prep Kit, Illumina HiSeq2000 and Illumina HiSeq4000) was performed. Strand specific RNA-seq libraries were generated which yielded a mean of 20 million reads per sample. Data from both Illumina platforms were integrated and analyzed with the same in-house pipeline. RNA-seq reads were aligned using GSNAP [15] against GRCh37 (articular cartilage or GRCh38 (subchondral bone) using default parameters. Read abundances per sample was estimated using HTSeq count v0.11.1 [16]. Only uniquely mapping reads were used for estimating expression. The quality of raw reads was checked using MultiQC v1.7 [17]. The adaptors were clipped using Cutadapt v1.1 [18] applying default settings (min overlap 3, min length).

Differential expression analysis

Differential expression analysis was performed between OA endotype A and B and between preserved and lesioned subchondral bone using the DESeq2 R package, version 1.24.0 [19]. Endotype A or preserved tissue were set as the reference and to correct for multiple testing Benjamini-Hochberg method was used, as indicated by the false discovery rate (FDR), with a significance cutoff value of 0.05.

Spearman correlation

First, gene expression levels were normalized by performing variance-stabilizing transformation using DESeq2 R package. Subsequently, Spearman correlations between gene expression levels and previously reported factor loading scores were calculated using Hmisc R package. Again Benjamini-Hochberg method was used to correct for multiple testing, as indicated by FDR.

Association between radiographic phenotypes and gene expression levels

Generalized estimation equation was performed in SPSS v25 to calculate association, with gene expression as dependent variable and sex, age, joint site and BMI as covariates.

Scoring of radiographic phenotypes joint space narrowing and osteophyte scores were described previously [11].

Results

Sample characteristics

The current study includes mRNA-seq data of 66 patients (N=56 articular cartilage samples, N=24 subchondral bone samples) who underwent a total joint replacement surgery due to OA (RAAK-study). As shown in **Figure 1**, of 14 patients both articular cartilage and subchondral bone mRNA-seq data were available. Of these 14 patients, 11 patients were assigned to OA endotype A, representing chondrocyte hypertrophy pathway while 3 patients were assigned to OA endotype B, representing immune response pathway and being associated to increased joint space narrowing in our previous study [11]. Data of these 14 patients were used to characterize the subchondral bone. Patients characteristics are shown in **Supplementary Table 1**.

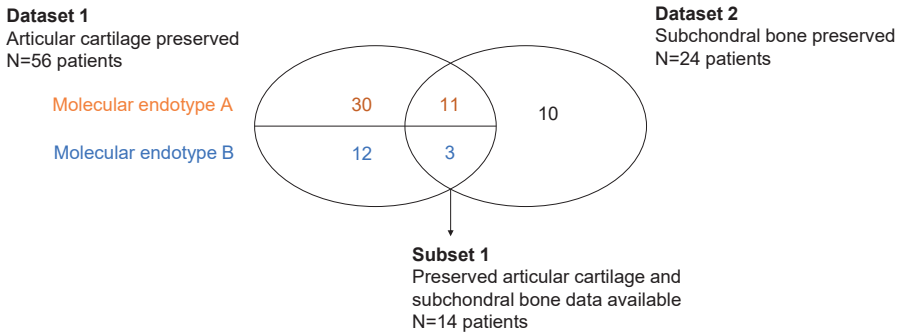

Figure 1 – Venn diagram of datasets used in this study.
Dataset 1 consists of preserved OA articular cartilage mRNA-seq data of 56 patients of whom endotypes were determined previously. Dataset 2 consists of preserved OA subchondral bone mRNA-seq data of 24 patients. Of 14 patients both articular cartilage and subchondral bone mRNA-seq data was available, indicated with subset 1.

Differential expression analysis between OA molecular endotype A and B subchondral bone

To evaluate whether the underlying subchondral bone showed differences between molecular endotype A and B identified in cartilage, we first compared transcriptomic profiles of macroscopically preserved subchondral bone between these endotypes (N=11 and N=3 paired samples for endotype A and B, respectively. **Subset 1, Figure 1**). Upon performing differential expression analysis, we identified 543 FDR significantly differentially expressed genes (**Supplementary Table 2**), of which 363 genes showed an absolute fold difference of 2 or higher. The most significantly upregulated gene in

endotype A relative to endotype B was *CHRDL2* (FD= 34.84, FDR= $3.37x10^{-2}$), while the most significantly upregulated gene in endotype B relative to endotype A was *BCL2L15* (FD= 22.17, FDR= $4,65x10^{-3}$). To see whether these differentially expressed genes were involved in particular pathways or processes, we performed gene enrichment analysis. Among the 94 genes upregulated in endotype A relative to endotype B, we only found significant enrichment for positive regulation of transcription from RNA polymerase II promoter (GO:0045944, 16 genes, FDR=$1.21x10^{-2}$), characterized by *NFAT5* (FD=1.67, FDR=$4.23x10^{-3}$) and *KLF15* (FD=2.98, FDR=$3.28x10^{-2}$) (**Supplementary Table 3A**). Among the 449 genes upregulated in endotype B relative to endotype A subchondral bone, we found significant enrichment for 32 processes, including immune response (GO:0006955, 34 genes, FDR=$5.30x10^{-6}$), characterized by expression of *IL1B* (FD=3.98, FDR=$4.11x10^{-3}$), *TNFSF14* (FD=7.48, FDR=$1.44x10^{-2}$), and *OSM* (FD=6.31 FDR=$1.19x10^{-4}$), and positive regulation of interleukin-6 production (GO:0032755, 16 genes, FDR=$2.19x10^{-5}$), characterized by expression of *IL1B* (FD=3.98, FDR=$4.11x10^{-3}$), *TNFSF4* (FD=2.37, FDR=$4.04x10^{-2}$), and *AIF1* (FD=2.53, FDR=$6.22x10^{-3}$), both processes also enriched among genes differentially expressed between OA endotypes in articular cartilage (**Supplementary Table 3B**).

Endotype A and B exclusive genes with OA pathophysiology in subchondral bone

Next, we explored the OA pathophysiological process in both OA molecular endotypes by comparing gene expression levels of macroscopically preserved and lesioned OA subchondral bone. Upon performing differential expression analysis between preserved and lesioned subchondral bone samples of patients with endotype A OA, we identified 107 genes FDR significantly differentially expressed (**Supplementary Table 4**). Of these genes, 15 genes showed an absolute foldchange of 2 or higher, including neuronal markers *STMN2* (FC=24.40 FDR=$1.52x10^{-2}$), *FGF14* (FC=0.32, FDR=$7.73x10^{-4}$), and *CNTNAP2* (FC=2.60, FDR=$1.50x10^{-2}$). We did not find significantly enriched processes among the differentially expressed genes. Differential expression analysis between preserved and lesioned subchondral bone of patients with endotype B OA resulted in identification of 11 genes being FDR significantly differentially expressed, of which 7 showed an absolute foldchange of 2 or higher (**Supplementary Table 5**). These differentially expressed genes included *COL1A1* (FC=2.26, FDR=$6.52x10^{-4}$), *GDF6* (FC=16.69, FDR=$2.27x10^{-2}$), and *CXCL9* (FC=0.30, FDR=$8.56x10^{-4}$). Gene enrichment analysis on these 11 differentially expressed genes showed significant enrichment for extracellular region and collagen type 1 trimer.

As shown in **Figure 2**, we identified 30 genes being exclusive for OA endotype A, i.e. not differentially expressed in OA endotype B nor in the total dataset [13], including *MYOC* (FC=0.15, FDR=$1.93x10^{-2}$), *CNTFR* (FC=0.51, .FDR=$1.31x10^{-2}$), and *CIC* (FC=0.74, FDR=$3.84x10^{-2}$). Moreover, we identified 7 genes exclusive for OA endotype B, i.e. not

differentially expressed in OA endotype A nor in the total dataset, including *COL1A1* (FC=2.26, FDR=6.52x10^{-4}), *COL1A2* (FC=1.89, FDR=3.46x10^{-2}), and *GDF6* (FC=16.69, FDR=2.27x10^{-2}).

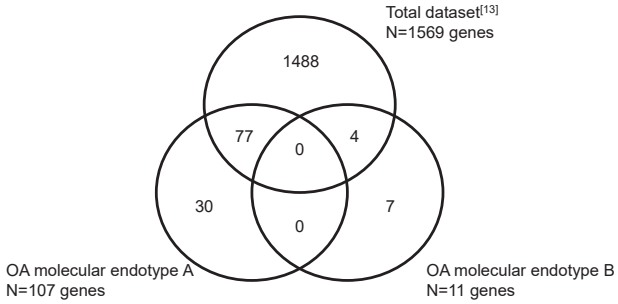

Figure 2 – Venn diagram of genes differentially expressed between preserved and lesioned OA subchondral bone in the total dataset, OA endotype A, and OA endotype B.
We identified 30 genes being exclusively differentially expressed in OA endotype A and 7 genes being exclusively differentially expressed in OA endotype B.

Markers for OA molecular endotype in subchondral bone

To find genes expressed in subchondral bone that mark OA endotype A or B, we calculated Spearman correlations between gene expression levels of the here identified genes differentially expressed between endotype A and B and previously reported quantitative factor loading scores representing contribution of each patient to either endotype A or B (N=14 patients, of whom RNA-seq data of subchondral bone and factor loading scores were available). Albeit not FDR significant, we found 36 genes correlating to these factor loading scores ($|\rho|>0.6$, P-value <0.05, **Table 1**).

Since radiographic OA feature joint space narrowing was previously shown to be higher in endotype B compared to endotype A patients, we calculated association between the 36 correlating genes and these radiographic phenotype scores (N=24 patients of whom RNA-seq data and radiographic phenotypes were available). As shown in **Table 1**, *RSP7P1, NSA2,* and *AC023090.2* were positively associated to joint space narrowing score, while *ZFP41* and *NOTCH4* were negatively associated to joint space narrowing score. All positively associated genes were higher expressed in endotype B, except for *AC023090.2*, while all negatively associated genes were lower expressed in endotype B compared to endotype A. This again confirms endotype B being associated to increased joint space narrowing. Together, these results show that high expression levels of *RSP7P1* and *NSA2* and low expression of *ZFP41* and *NOTCH4* characterize endotype B OA in subchondral bone.

Comparison subchondral bone and articular cartilage

To find genes that mark OA molecular endotypes A and B in both articular cartilage and subchondral bone, we compared the results of subchondral bone presented here with our previously reported results on articular cartilage [11]. Upon comparing genes that were differently expressed between endotype A and B in both tissues, we found 185 genes overlapping, of which 180 genes showed similar directions of effect, including *PLAUR, CHRDL2*, and *NOTCH4* (**Supplementary Figure 1A, Supplementary Table 6**). These 180 genes were significantly enriched for 46 processes (**Supplementary Table 7**). Of these 46 processes, 45 were involved in processes regarding immune response, represented by genes such as *IL1B, OSM,* and *CD38*.

Upon comparing the exclusively molecular endotype A and B differentially expressed genes between preserved and lesioned subchondral bone and articular cartilage, we found 3 genes exclusively differentially expressed in molecular endotype A in both subchondral bone and articular cartilage (**Supplementary Figure 1B, Supplementary Table 8**). We did not find any overlapping genes between bone and cartilage in molecular endotype B exclusive genes (**Supplementary Figure 1C**).

Discussion

In the current study, we characterized the underlying bone of previously identified consistent OA molecular endotypes (endotype A and endotype B) in articular cartilage. Upon comparing gene expression levels of the underlying subchondral bone between the molecular endotypes identified in articular cartilage, we found 543 genes being FDR significantly differentially expressed. Compared to findings in articular cartilage, these 543 differentially expressed genes were enriched for similar processes, including immune response (GO:0006955) and signal transduction (GO:0007165). Subsequently, upon performing differential expression analysis between preserved and lesioned OA subchondral bone stratified for OA molecular endotype, we identified 30 FDR significantly differently expressed genes exclusively for endotype A and 7 FDR significantly differentially expressed genes exclusively for endotype B.

Although OA molecular endotype A and B robustly identified in articular cartilage were not previously identified in subchondral bone, we here showed that underlying subchondral bone is different between OA endotypes. Upon performing differential expression analysis between preserved and lesioned OA subchondral bone stratified for OA endotype, we identified 107 genes FDR significantly differentially expressed for endotype A. Among these genes we found neuronal markers *CNTNAP2* and *STMN2,* which were both increased in lesioned OA subchondral bone (FC=2.60 and FC=24.40, respectively) [20-23]. This could suggest that new neuronal structures are formed with OA in patients with endotype A OA, resulting in more pain compared to patients with

Table 1 – association between genes marking endotype A and B OA in subchondral bone and radiographic phenotype joint space narrowing.
RSP7P1, *NSA2*, and *AC023090.2* showed positive association to JSN scores and were higher expressed in endotype B compared to endotype A patients, except for *AC023090.2*. *ZFP41* and *NOTCH4* were negatively associated to JSN and were higher expressed in endotype A compared to endotype B OA patients. Correlation between gene expression and FLS was calculated using data of 14 patients and association between gene expression and joint space narrowing scores was calculated using data of 24 patients.

	Joint space narrowing score				Correlation FLS		Fold difference
Gene	b	lower	upper	p-value	ρ	p-value	B vs A
SVBP	-0.03	-0.12	0.05	3.99E-01	0.72	3.78E-03	1.61
RIT1	-0.01	-0.06	0.04	7.19E-01	0.71	4.45E-03	1.41
ELOF1	0.01	-0.04	0.06	6.89E-01	0.71	4.82E-03	1.50
RPS24P8	0.03	0.00	0.07	6.13E-02	0.70	5.63E-03	1.51
LYSMD2	0.02	-0.04	0.08	4.87E-01	0.68	7.04E-03	1.50
IL1B	0.10	-0.02	0.22	9.32E-02	0.68	7.56E-03	3.98
AC004453.1	0.06	-0.02	0.14	1.43E-01	0.67	8.70E-03	1.44
CYREN	0.02	-0.04	0.08	5.65E-01	0.67	8.70E-03	1.49
AL450405.1	-0.04	-0.11	0.04	3.54E-01	0.67	9.32E-03	1.41
RPS7P1	**0.04**	**0.00**	**0.08**	**4.54E-02**	**0.65**	1.21E-02	**1.49**
TNFSF4	0.04	-0.04	0.11	3.37E-01	0.64	1.29E-02	2.37
ID2	0.03	-0.09	0.15	6.23E-01	0.63	1.56E-02	1.35
TUBAP2	0.01	-0.06	0.07	8.67E-01	0.63	1.56E-02	2.42
OST4	-0.04	-0.09	0.00	8.08E-02	0.63	1.65E-02	1.48
ANAPC11	-0.03	-0.08	0.02	2.13E-01	0.62	1.76E-02	1.51
TUBA1C	0.00	-0.08	0.07	9.79E-01	0.62	1.76E-02	2.09
CENPK	0.00	-0.07	0.07	9.29E-01	0.62	1.86E-02	3.65
NSA2	**0.06**	**0.02**	**0.10**	**6.10E-03**	**0.61**	1.97E-02	**1.47**
GAPDHP1	-0.07	-0.15	0.01	8.25E-02	0.61	2.09E-02	1.87
TMEM9B	-0.01	-0.04	0.02	5.29E-01	0.61	2.09E-02	1.48
EEF1B2	0.06	-0.01	0.12	8.25E-02	0.60	2.21E-02	1.74
AL590999.1	0.05	-0.01	0.11	1.12E-01	-0.60	2.21E-02	0.32
AC068587.4	0.02	-0.22	0.27	8.53E-01	-0.61	2.09E-02	0.25
ZFP41	**-0.08**	**-0.14**	**-0.02**	**1.23E-02**	**-0.62**	1.86E-02	**0.46**
FAM214A	0.02	-0.03	0.08	3.98E-01	-0.62	1.76E-02	0.65
NALT1	-0.06	-0.19	0.07	3.77E-01	-0.63	1.56E-02	0.20
ZNF580	-0.04	-0.10	0.03	2.49E-01	-0.63	1.56E-02	0.56
TTC28	-0.03	-0.13	0.06	4.70E-01	-0.64	1.47E-02	0.51
KIAA1217	-0.05	-0.16	0.06	3.63E-01	-0.65	1.14E-02	0.49
KAT2A	-0.03	-0.09	0.04	3.98E-01	-0.66	1.07E-02	0.66
USP31	0.00	-0.05	0.05	9.16E-01	-0.66	9.98E-03	0.63
ZNF703	-0.06	-0.19	0.06	2.91E-01	-0.67	9.32E-03	0.35

AC023090.2	**0.05**	**0.01**	**0.08**	**1.58E-02**	**-0.67**	8.70E-03	**0.21**
NOTCH4	**-0.14**	**-0.22**	**-0.07**	**1.33E-04**	**-0.69**	6.07E-03	**0.54**
KLF15	0.07	-0.02	0.16	1.27E-01	-0.75	1.84E-03	0.34
CNTN2	-0.03	-0.15	0.10	6.84E-01	-0.83	2.51E-04	0.18

endotype B OA, which is in line with the fact that patients of endotype A have wide joint spaces, hence cartilage, at the moment of their total joint replacement surgery. Upon comparing preserved and lesioned OA subchondral bone in endotype B OA, we identified 11 FDR significant differentially expressed genes. Among these 11 genes we identified *COL1A1* (FC=2.26) , *COL1A2* (FC=1.88), *CXCL9* (FC=0.30), and *GDF6* (FC=16.69). *CXCL9*, encoding C-X-C motif chemokine ligand 9, was previously shown to inhibit bone formation and promoting bone resorption, resulting in bone loss [24]. *GDF6,* encoding growth differentiation factor 6, is required for normal formation of joints and bone [25, 26]. Upregulation of *COL1A1, COL1A2,* and *GDF6,* together with downregulation of *CXCL9* suggests capacity of bone formation with ongoing OA in endotype B patients, which is in line with observed increased joint space narrowing. It is tempting to speculate that this bone forming capacity prevents pain sensation in these endotype B patients.

In our previous study in which we performed cluster analysis based on top 1000 most variable genes expressed in subchondral bone, we identified clusters based on joint site but no clustering similar to identified OA molecular endotype A and B in articular cartilage [13]. This suggests that the difference between hip and knee subchondral bone is probably larger than the difference between OA endotypes. Therefore, a larger dataset is required to be able to identify OA endotypes in subchondral bone. Moreover, optimizing the number of variable genes included in the cluster analysis could also result in identification of these OA endotypes. As such, the main drawback of current study is the relatively low sample size and small overlap between subchondral bone and articular cartilage samples (N=14 patients: N=11 endotype A, N=3 endotype B). Nevertheless, despite this low sample size we were able to identify FDR significantly differentially expressed genes, indicating their consistency in expression. Increasing sample size and overlap between articular cartilage and subchondral bone might result in the identification of more genes and pathways and therefore better characterization. Validation of the results reported here in an independent dataset is necessary.

Altogether, we here showed that underlying bone of OA endotypes identified in articular cartilage is significantly different between endotypes. We showed that OA endotype B was associated with bone formation capacity, in line with increased joint space narrowing. Moreover, OA endotype A was associated with increased expression

of neuronal markers, suggesting these patients might experience pain in an earlier OA stage compared to endotype B OA patients.

Declarations

Acknowledgements

We thank all the participants of the RAAK study. The LUMC has and is supporting the RAAK study. We thank Robert van der Wal, Demiën Broekhuis, Anika Rabelink-Hoogenstraaten, Peter van Schie, Shaho Hasan, Maartje Meijer, Daisy Latijnhouwers and Geert Spierenburg for collecting the RAAK material. We thank the Sequence Analysis Support Core (SASC) of the Leiden University Medical Center for their support. Data is generated within the scope of the Medical Delta programs Regenerative Medicine 4D: Generating complex tissues with stem cells and printing technology and Improving Mobility with Technology.

Funding

The study was funded by the Dutch Scientific Research council NWO /ZonMW VICI scheme (nr 91816631/528), Foundation for Research in Rheumatology (FOREUM), BBMRI-NL complementation project CP2013-83, Ana Fonds (O2015-27), and TreatOA (grant 200800 from the European Commission Seventh Framework Program).

Disclosures

The authors have declared no conflicts of interest.

References

1. Li, G., et al., *Subchondral bone in osteoarthritis: insight into risk factors and microstructural changes.* Arthritis Research & Therapy, 2013. **15**(6): p. 223.
2. Glyn-Jones, S., et al., *Osteoarthritis.* Lancet, 2015. **386**(9991): p. 376-87.
3. Fellows, C.R., C. Matta, and A. Mobasheri, *Applying Proteomics to Study Crosstalk at the Cartilage-Subchondral Bone Interface in Osteoarthritis: Current Status and Future Directions.* EBioMedicine, 2016. **11**: p. 2-4.
4. Goldring, S.R. and M.B. Goldring, *Changes in the osteochondral unit during osteoarthritis: structure, function and cartilage-bone crosstalk.* Nat Rev Rheumatol, 2016. **12**(11): p. 632-644.
5. Funck-Brentano, T. and M. Cohen-Solal, *Crosstalk between cartilage and bone: when bone cytokines matter.* Cytokine Growth Factor Rev, 2011. **22**(2): p. 91-7.
6. Pan, J., et al., *Elevated cross-talk between subchondral bone and cartilage in osteoarthritic joints.* Bone, 2012. **51**(2): p. 212-7.
7. Boer, C.G., et al., *Deciphering osteoarthritis genetics across 826,690 individuals from 9 populations.* Cell, 2021.
8. Ghouri, A. and P.G. Conaghan, *Update on novel pharmacological therapies for osteoarthritis.* Ther Adv Musculoskelet Dis, 2019. **11**: p. 1759720x19864492.
9. Grässel, S. and D. Muschter, *Recent advances in the treatment of osteoarthritis.* F1000Research, 2020. **9**: p. F1000 Faculty Rev-325.
10. Soul, J., et al., *Stratification of knee osteoarthritis: two major patient subgroups identified by genome-wide expression analysis of articular cartilage.* Ann Rheum Dis, 2018. **77**(3): p. 423.
11. Coutinho de Almeida, R., et al., *Identification and characterization of two consistent osteoarthritis subtypes by transcriptome and clinical data integration.* Rheumatology (Oxford), 2020.
12. Coutinho de Almeida, R., et al., *RNA sequencing data integration reveals an miRNA interactome of osteoarthritis cartilage.* Ann Rheum Dis, 2019. **78**(2): p. 270-277.
13. Tuerlings, M., et al., *RNA sequencing reveals interacting key determinants of osteoarthritis acting in subchondral bone and articular cartilage.* Arthritis Rheumatol, 2020.
14. Ramos, Y.F., et al., *Genes involved in the osteoarthritis process identified through genome wide expression analysis in articular cartilage; the RAAK study.* PLoS One, 2014. **9**(7): p. e103056.
15. Wu, T.D. and C.K. Watanabe, *GMAP: a genomic mapping and alignment program for mRNA and EST sequences.* Bioinformatics, 2005. **21**(9): p. 1859-75.
16. Anders, S., P.T. Pyl, and W. Huber, *HTSeq--a Python framework to work with high-throughput sequencing data.* Bioinformatics, 2015. **31**(2): p. 166-9.
17. Ewels, P., et al., *MultiQC: summarize analysis results for multiple tools and samples in a single report.* Bioinformatics, 2016.

32(19): p. 3047-8.
18. Martin, M., *Cutadapt removes adapter sequences from high-throughput sequencing reads.* 2011, 2011. **17**(1): p. 3 %J EMBnet.journal.
19. Love, M.I., W. Huber, and S. Anders, *Moderated estimation of fold change and dispersion for RNA-seq data with DESeq2.* Genome Biology, 2014. **15**(12): p. 550.
20. Lu, Z., et al., *Molecular Architecture of Contactin-associated Protein-like 2 (CNTNAP2) and Its Interaction with Contactin 2 (CNTN2).* J Biol Chem, 2016. **291**(46): p. 24133-24147.
21. Rodenas-Cuadrado, P., J. Ho, and S.C. Vernes, *Shining a light on CNTNAP2: complex functions to complex disorders.* Eur J Hum Genet, 2014. **22**(2): p. 171-8.
22. Chiellini, C., et al., *Stathmin-like 2, a developmentally-associated neuronal marker, is expressed and modulated during osteogenesis of human mesenchymal stem cells.* Biochem Biophys Res Commun, 2008. **374**(1): p. 64-8.
23. Kuttapitiya, A., et al., *Microarray analysis of bone marrow lesions in osteoarthritis demonstrates upregulation of genes implicated in osteochondral turnover, neurogenesis and inflammation.* Ann Rheum Dis, 2017. **76**(10): p. 1764-1773.
24. Liu, Z., et al., *Increased Osteoblastic Cxcl9 Contributes to the Uncoupled Bone Formation and Resorption in Postmenopausal Osteoporosis.* Clinical interventions in aging, 2020. **15**: p. 1201-1212.
25. Deng, P., et al., *Growth differentiation factor 6, a repressive target of EZH2, promotes the commitment of human embryonic stem cells to mesenchymal stem cells.* Bone Research, 2020. **8**(1): p. 39.
26. Settle, S.H., Jr., et al., *Multiple joint and skeletal patterning defects caused by single and double mutations in the mouse Gdf6 and Gdf5 genes.* Dev Biol, 2003. **254**(1): p. 116-30.

Supplementary files

Supplementary figures

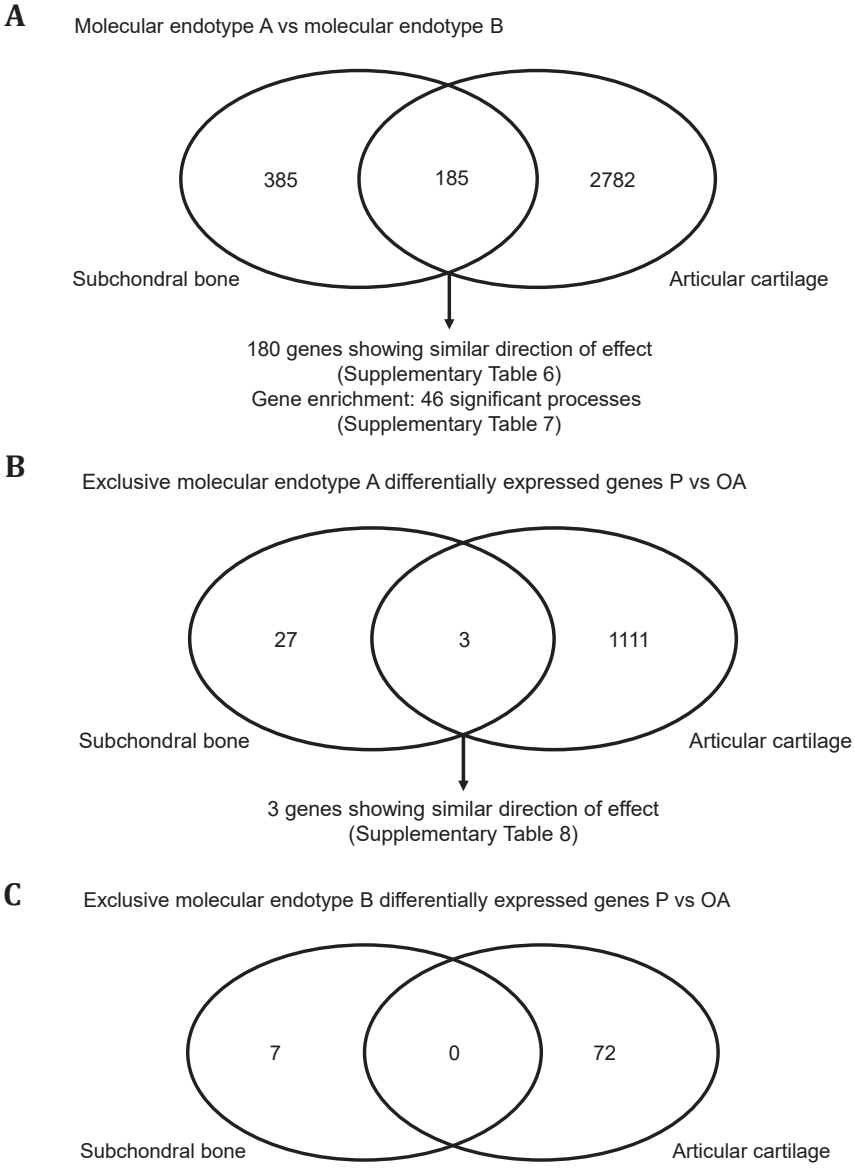

Supplementary Figure 1 – Venn diagrams representing overlapping genes between subchondral bone and articular cartilage.
(A) Overlapping genes differentially expressed between OA molecular endotype A and B in articular cartilage and subchondral bone. (B) Overlapping differentially expressed genes between preserved and lesioned articular cartilage and subchondral bone exclusive for molecular endotype A. (C) Overlapping differentially expressed genes between preserved and lesioned articular cartilage and subchondral bone exclusive for molecular endotype B.

Supplementary tables

Supplementary Table 1 – patient characteristics

	Cartilage samples (N=56)	Bone samples (N=24)	Overlap cartilage and bone (N=14)
mean age (stdev)	68.0 (8.4)	66.2 (8.6)	67 (8.9)
female (male)	45 (11)	22 (2)	12 (2)
knees (hips)	35 (21)	18 (6)	12 (2)

Supplementary Table 2 (partially) - Differentially expressed genes in macroscopically preserved subchondral bone between OA endotype A and B.
Subtype A is set as a reference. The top 50 most significant differentially expressed genes between OA endotype A and B are shown here.

Ensembl ID	Gene Name	Base mean	Log 2 fold change	Fold change	P-value	FDR
ENSG00000198829	SUCNR1	68.00	2.61	6.10	1.31E-08	1.19E-04
ENSG00000099985	OSM	13.00	2.66	6.31	1.39E-08	1.19E-04
ENSG00000101916	TLR8	87.89	2.19	4.57	6.80E-08	3.88E-04
ENSG00000204482	LST1	145.88	2.64	6.24	4.06E-07	1.60E-03
ENSG00000100427	MLC1	64.30	4.29	19.51	4.68E-07	1.60E-03
ENSG00000118640	VAMP8	136.50	1.57	2.97	1.22E-06	3.28E-03
ENSG00000087586	AURKA	50.22	3.21	9.26	1.61E-06	3.28E-03
ENSG00000173391	OLR1	55.34	3.95	15.45	1.72E-06	3.28E-03
ENSG00000131355	ADGRE3	25.53	4.17	18.01	1.45E-06	3.28E-03
ENSG00000111639	MRPL51	216.99	0.61	1.53	3.46E-06	3.49E-03
ENSG00000274210	RF00003	80.59	1.71	3.28	2.69E-06	3.49E-03
ENSG00000116701	NCF2	397.12	2.04	4.10	2.93E-06	3.49E-03
ENSG00000146285	SCML4	13.29	2.16	4.47	2.83E-06	3.49E-03
ENSG00000150681	RGS18	110.25	2.50	5.65	2.62E-06	3.49E-03
ENSG00000105374	NKG7	128.09	2.98	7.88	3.30E-06	3.49E-03
ENSG00000214212	C19orf38	48.88	3.15	8.89	3.36E-06	3.49E-03
ENSG00000163563	MNDA	423.31	3.47	11.10	2.40E-06	3.49E-03
ENSG00000090382	LYZ	3397.50	4.02	16.19	3.72E-06	3.54E-03
ENSG00000123329	ARHGAP9	160.76	2.32	5.00	4.10E-06	3.70E-03
ENSG00000116586	LAMTOR2	99.12	0.68	1.60	4.86E-06	4.11E-03
ENSG00000125538	IL1B	14.23	1.99	3.98	5.04E-06	4.11E-03
ENSG00000149328	GLB1L2	136.66	-1.92	0.26	5.91E-06	4.23E-03
ENSG00000102908	NFAT5	1401.35	-0.74	0.60	6.17E-06	4.23E-03
ENSG00000120280	CXorf21	48.52	1.89	3.70	6.01E-06	4.23E-03
ENSG00000072274	TFRC	1625.28	3.00	7.98	6.14E-06	4.23E-03
ENSG00000111348	ARHGDIB	1126.50	2.10	4.30	6.83E-06	4.50E-03
ENSG00000224578	HNRNPA1P48	204.31	0.89	1.85	7.26E-06	4.60E-03
ENSG00000160883	HK3	197.06	3.62	12.26	7.53E-06	4.61E-03
ENSG00000188761	BCL2L15	20.18	4.47	22.17	7.87E-06	4.65E-03
ENSG00000151725	CENPU	49.02	3.14	8.81	8.39E-06	4.79E-03
ENSG00000187116	LILRA5	44.28	3.33	10.04	9.45E-06	5.22E-03

Ensembl ID	Gene Name	Base mean	Log 2 fold change	Fold change	P-value	FDR
ENSG00000170312	CDK1	83.29	2.68	6.41	9.94E-06	5.32E-03
ENSG00000145569	OTULINL	155.75	1.31	2.47	1.15E-05	5.78E-03
ENSG00000132965	ALOX5AP	197.85	2.71	6.55	1.15E-05	5.78E-03
ENSG00000169429	CXCL8	47.25	2.49	5.60	1.19E-05	5.83E-03
ENSG00000138160	KIF11	98.56	3.48	11.19	1.26E-05	5.99E-03
ENSG00000102445	RUBCNL	70.34	1.13	2.19	1.31E-05	6.08E-03
ENSG00000175348	TMEM9B	208.68	0.57	1.48	1.49E-05	6.22E-03
ENSG00000213261	EEF1B2P6	21.33	1.13	2.18	1.47E-05	6.22E-03
ENSG00000204472	AIF1	219.86	1.34	2.53	1.48E-05	6.22E-03
ENSG00000174837	ADGRE1	22.89	2.95	7.71	1.47E-05	6.22E-03
ENSG00000105383	CD33	112.33	1.23	2.35	1.79E-05	6.27E-03
ENSG00000155629	PIK3AP1	471.28	1.28	2.43	1.74E-05	6.27E-03
ENSG00000163154	TNFAIP8L2	48.58	1.85	3.61	1.70E-05	6.27E-03
ENSG00000165168	CYBB	1795.73	1.94	3.83	1.78E-05	6.27E-03
ENSG00000111679	PTPN6	297.26	1.95	3.87	1.68E-05	6.27E-03
ENSG00000100365	NCF4	239.96	2.04	4.12	1.64E-05	6.27E-03
ENSG00000166501	PRKCB	214.73	2.28	4.86	1.75E-05	6.27E-03
ENSG00000084110	HAL	32.42	3.23	9.40	1.76E-05	6.27E-03
ENSG00000158321	AUTS2	242.66	-1.12	0.46	1.87E-05	6.28E-03

Supplementary Table 3 – Gene enrichment on genes differentially expressed between OA molecular endotype A and B.
Supplementary Table 3A- Gene enrichment of genes upregulated in endotype A relative to endotype B subchondral bone

GO-Term	Count	%	P-value	FDR	Genes
GO:0045944~positive regulation of transcription from RNA polymerase II promoter	16	20	2.22E-05	1.21E-02	ZFP64, SALL4, NFAT5, GLI3, ZMIZ1, KAT2A, ZBTB16, LPIN3, CRTC3, ZFHX3, NFIC, AUTS2, KLF15, ATF7, TNKS, ZNF580

Supplementary Table 3B- Gene enrichment of genes upregulated in endotype B relative to endotype A subchondral bone

GO-Term	Count	%	P-value	FDR	Genes
GO:0005886~plasma membrane	169	39	1.12E-12	4.72E-10	M6PR, CD38, LAMP2, BTK, PLAUR, TYROBP, ACPP, WAS, DEF6, CYBA, SLC2A3, GNA15, YBX1, DAPP1, CDC42, TFRC, ANKRD13A, ICAM3, STXBP2, PTPRC, FYB1, PILRA, LAT2, SRPK1, CYTH4, GRAP2, CSF2RB, MLC1, RASSF2, SIRPB1, HCK, TLR8, RP2, CORO1A, AQP9, CD37, LILRB1, ICAM4, NKG7, CD33, PIK3CG, BIN2, CLEC4A, TREML2, ITGA4, GCA, IL18RAP, PLEK, LAMTOR2, RAB29, TNFSF4, LRMP, VAMP8, ADCY7, CCRL2, CD244, ARL4A, CLTA, NCKAP1L, PTGER2, OPRL1, TNFSF14, VASP, HCST, CFP, YWHAH, RAC2, LRRC4, ATP8B3, MPP1, LILRB2, SH3BGRL, CAP1, ADGRE3, CD180, DOCK2, USP15, PLXNC1, LCP1, MYO1G, GYPC, CASP1, GPR84, GPR65, PSTPIP1, IGSF6, ARRB2, VAV1, MYO1F, SIGLEC10, SLC2A5, EFHD2, CD53, RIT1, RALB, PAK1, LAMTOR1, RGS18, ADAM8, ARL11, PSTPIP2, PIP4P2, PIK3AP1, CD1C, FCER1G, JAML, FCGR3B, CXCR1, CIP2A, CD200R1, PLB1, F2RL1, SYK, CYBB, MELK, PRKCB, CLEC4D, STX3, NOD2, SNX20, CD300A, RGS14, SLC50A1, PTAFR, CD52, REPS2, UBB, EMB, OSCAR, CEACAM3, FPR1, RGS19, HDAC3, RAB37, OLR1, TNFRSF10C, TLR1, ADGRE1, TBC1D10C, KCNE3, P2RY2, GAPT, CRLF3, CD300LB, ZNRF2, CXCR2, EVI2B, CD300LF, CD300E, HYAL3, LILRA5, SELL, SEMA4A, SIRPB2, C5AR1, SLC28A3, MBP, SUCNR1, CHML, LST1, LILRB3, IGLV1-40, IGLV3-21, GPSM3, UBA52, LTB, NFAM1, LILRA6, LYN
GO:0006955~immune response	34	8	2.34E-09	5.30E-06	WAS, LCP2, FYB1, OSM, TLR8, PIK3CG, CLEC4A, IL18RAP, TNFSF4, CCRL2, IL1B, TNFSF14, CFP, LILRB2, GPR65, IGSF6, VAV1, CD1C, FCGR3B, CTSS, CXCR1, CLEC4D, PTAFR, CXCL8, CTSW, TLR1, CXCR2, C5AR1, MBP, LST1, IGLV1-40, IGLV3-21, GPSM3, LTB
GO:0030667~secretory granule membrane	17	4	9.93E-09	1.49E-06	CD38, TYROBP, SLC2A3, RAB27A, PTPRC, SIRPB1, VAMP8, NCKAP1L, ADGRE3, FCGR3B, CXCR1, PTAFR, FPR1, CXCR2, SELL, C5AR1, LILRB3

GO-Term	Count	%	P-value	FDR	Genes
GO:0070821~tertiary granule membrane	15	3	1.06E-08	1.49E-06	CYBA, SLC2A3, CD33, LAMTOR2, VAMP8, LILRB2, GPR84, CD53, ADAM8, FCER1G, CYBB, CLEC4D, CD300A, PTAFR, OLR1
GO:0032755~positive regulation of interleukin-6 production	16	4	2.77E-08	2.19E-05	BTK, TYROBP, CYBA, TLR8, PYCARD, TNFSF4, IL1B, LILRB2, F2RL1, SYK, NOD2, PTAFR, TLR1, LILRA5, MBP, AIF1
GO:0006954~inflammatory response	31	7	2.90E-08	2.19E-05	CYBA, LYZ, NLRC4, HCK, TLR8, PYCARD, NKG7, PIK3CG, IL18RAP, TNFSF4, CCRL2, PTGER2, IL1B, CD180, PSTPIP1, ADAM8, GBP5, PROK2, F2RL1, CYBB, AD000864.1, PTAFR, CXCL8, FPR1, OLR1, TLR1, CXCR2, HYAL3, C5AR1, AIF1, NFAM1
GO:0035579~specific granule membrane	16	4	7.12E-08	7.53E-06	PLAUR, CYBA, SLC2A3, CD33, LAMTOR2, VAMP8, GPR84, SLC2A5, CD53, LAMTOR1, ADAM8, CYBB, CLEC4D, CEACAM3, RAB37, OLR1
GO:0101003~ficolin-1-rich granule membrane	12	3	6.29E-07	5.32E-05	LAMP2, SLC2A3, NCKAP1L, LILRB2, ADGRE3, LAMTOR1, ADAM8, FCER1G, CLEC4D, CD300A, FPR1, TBC1D10C
GO:0007165~signal transduction	56	13	8.67E-07	4.91E-04	CD38, PLAUR, TYROBP, GDI2, DAPP1, ARHGAP15, PILRA, ARHGAP4, GRAP2, CSF2RB, RASSF2, SIRPB1, PYCARD, LILRB1, CD33, TNFSF4, STMN1, RPS6KA1, CD244, ARHGAP9, IL1B, TNFSF14, YWHAH, RAC2, GMFG, MPP1, LILRB2, CAP1, OSTF1, STAM, CASP1, PSTPIP1, CMTM2, COPS3, ARRB2, CD53, RIT1, RALB, RACGAP1, ARHGAP25, CD200R1, TAGAP, PRKCB, CXCL8, CEACAM3, FPR1, MOB1B, TLR1, ERFE, CXCR2, ARHGAP30, C5AR1, LTB, NFAM1, LYN, RASSF5
GO:0030593~neutrophil chemotaxis	11	3	3.68E-06	1.67E-03	PIK3CG, NCKAP1L, IL1B, VAV1, FCER1G, JAML, CXCR1, SYK, CXCL8, CXCR2, C5AR1
GO:0050790~regulation of catalytic activity	27	6	1.06E-05	4.00E-03	BTK, WAS, DEF6, GDI2, ACAP1, ARHGAP4, CYTH4, NCF4, SEC23B, RP2, ARHGDIB, EEF1B2, LAMTOR2, NCF2, PSD4, RAC2, ALOX5AP, DOCK2, BMP2K, SAE1, LAMTOR1, RGS18, RACGAP1, TAGAP, ARHGAP30, CHML, GPSM3

GO-Term	Count	%	P-value	FDR	Genes
GO:0005887~integral component of plasma membrane	51	12	1.73E-05	1.22E-03	M6PR, PLAUR, TYROBP, SLC2A3, TFRC, ICAM3, PTPRC, CSF2RB, SIRPB1, AQP9, CD37, ICAM4, NKG7, CD33, CLEC4A, TNFSF4, LRMP, ADCY7, CCRL2, NCKAP1L, PTGER2, OPRL1, LILRB2, ADGRE3, PLXNC1, GYPC, GPR84, GPR65, IGSF6, SLC2A5, CD53, ADAM8, CD1C, FCER1G, FCGR3B, F2RL1, CYBB, PTAFR, EMB, OLR1, TLR1, ADGRE1, P2RY2, CXCR2, EVI2B, SELL, SEMA4A, C5AR1, SLC28A3, CHML, LILRB3
GO:0070062~extracellular exosome	84	20	2.04E-05	1.23E-03	CD38, LAMP2, ACPP, WAS, GDI2, SLC2A3, YBX1, RAB27A, CDC42, TFRC, ICAM3, STXBP2, VDAC3, PTPRC, PILRA, LAT2, LYZ, RP2, GLA, CORO1A, CD37, BLVRA, LTA4H, ARPC3, ARHGDIB, PTPN6, SNX3, ACTR3, ITGA4, GCA, QPCT, CAPZA1, RAB29, STMN1, VAMP8, GOT1, GLIPR2, NCKAP1L, VASP, YWHAH, RAC2, ARPC1B, SH3BGRL, CAP1, PCNA, DOCK2, LCP1, MYO1G, TXN, TOR1A, SLC2A5, CD53, TPM3, RALB, LAMTOR1, FAM49B, RACGAP1, ARPC5, FCGR3B, ARPC2, MNDA, TKT, H2AFZ, PRKCB, STX3, CD300A, CDK1, UBB, OSCAR, LRG1, CFL1, MOB1B, B3GNT8, GBA, ALYREF, HIST2H2BE, TUBB4B, HIST1H4J, SUCNR1, IGLV3-21, UBA52, LYN, HIST1H4K, PSMB3
GO:0050766~positive regulation of phagocytosis	9	2	2.14E-05	6.68E-03	BTK, CYBA, RAB27A, SIRPB1, PYCARD, IL1B, DOCK2, FCER1G, NOD2
GO:0032731~positive regulation of interleukin-1 beta production	10	2	2.36E-05	6.68E-03	TYROBP, NLRC4, TLR8, PYCARD, CASP1, GBP5, MNDA, F2RL1, NOD2, LILRA5
GO:0005102~receptor binding	22	5	4.09E-05	1.65E-02	PLAUR, TYROBP, ICAM3, PTPRC, FYB1, FCN1, HCK, GLA, TNFSF4, TNFSF14, HCST, MPP1, TESPA1, PLXNC1, CNPY3, ARRB2, PIK3AP1, F2RL1, SYK, GBA, LTB, LYN
GO:0032396~inhibitory MHC class I receptor activity	5	1	5.34E-05	1.65E-02	LILRB1, LILRB2, LILRA5, LILRB3, LILRA6
GO:0032757~positive regulation of interleukin-8 production	10	2	5.91E-05	1.49E-02	FCN1, TLR8, PYCARD, CD244, IL1B, LAMTOR5, F2RL1, SYK, NOD2, TLR1
GO:0045730~respiratory burst	6	1	6.55E-05	1.49E-02	CYBA, NCF4, NCF2, RAC2, CYBB, CD52

GO-Term	Count	%	P-value	FDR	Genes
GO:0006935~chemotaxis	12	3	8.45E-05	1.74E-02	PLAUR, CCRL2, NCKAP1L, RAC2, DOCK2, CMTM2, PROK2, PTAFR, CXCL8, FPR1, CXCR2, C5AR1
GO:0005576~extracellular region	62	14	1.00E-04	4.73E-03	PLAUR, ALOX5, GDI2, YBX1, RAB27A, TFRC, STXBP2, FCN1, LYZ, OSM, GLA, PYCARD, LILRB1, ICAM4, BIN2, LTA4H, ACRBP, PTPN6, GCA, QPCT, PLEK, CAPZA1, PLBD1, GLIPR2, ARHGAP9, IL1B, CFP, GMFG, CAP1, ADGRE3, DOCK2, OSTF1, AOAH, TXN, CASP1, SIGLEC10, FAM49B, HK3, ARPC5, FCGR3B, CTSS, PROK2, MNDA, CD200R1, GYG1, CXCL8, CD52, OSCAR, LRG1, CTSW, HPSE, OLR1, SVBP, ERFE, HYAL3, LILRA5, TUBB4B, HIST1H4J, TMSB4X, IGLV1-40, IGLV3-21, HIST1H4K
GO:0005885~Arp2/3 protein complex	5	1	1.01E-04	4.73E-03	ARPC3, ACTR3, ARPC1B, ARPC5, ARPC2
GO:0031623~receptor internalization	9	2	1.19E-04	1.96E-02	TFRC, LILRB1, ARRB2, RALB, FCER1G, CXCR1, SYK, CXCL8, CXCR2
GO:0002250~adaptive immune response	19	4	1.24E-04	1.96E-02	BTK, LAT2, LILRB1, PIK3CG, CLEC4A, CD244, LILRB2, SIGLEC10, CD1C, CTSS, SYK, PRKCB, CLEC4D, ADGRE1, LILRB3, IGLV1-40, IGLV3-21, LILRA6, LYN
GO:0032760~positive regulation of tumor necrosis factor production	12	3	1.27E-04	1.96E-02	BTK, TYROBP, CYBA, PTPRC, PYCARD, SASH3, SYK, CYBB, NOD2, PTAFR, TLR1, LILRA5
GO:0032729~positive regulation of interferon-gamma production	10	2	1.32E-04	1.96E-02	TLR8, PYCARD, LILRB1, TNFSF4, SASH3, CD244, IL1B, PTPN22, FAM49B, F2RL1
GO:0042102~positive regulation of T cell proliferation	9	2	1.38E-04	1.96E-02	TFRC, PTPRC, CORO1A, TNFSF4, SASH3, NCKAP1L, IL1B, LILRB2, AIF1
GO:0007186~G-protein coupled receptor signaling pathway	22	5	1.96E-04	2.62E-02	FCN1, PIK3CG, PTPN6, CCRL2, PTGER2, RAC2, ADGRE3, GPR65, VAV1, RGS18, PROK2, CXCR1, F2RL1, RGS14, PTAFR, CXCL8, FPR1, RGS19, ADGRE1, P2RY2, SUCNR1, CHML
GO:0045087~innate immune response	28	7	2.13E-04	2.67E-02	BTK, CYBA, NLRC4, SRPK1, HCK, RIOK3, TLR8, CORO1A, PYCARD, PIK3CG, CLEC4A, NCF2, CXorf21, CD244, CD180, CNPY3, PSTPIP1, SIGLEC10, FCER1G, TNFAIP8L2, F2RL1, SYK, CYBB, NOD2, TLR1, APOBEC3B, LILRA5, LYN
GO:0032733~positive regulation of interleukin-10 production	7	2	2.24E-04	2.67E-02	PYCARD, TNFSF4, SASH3, F2RL1, SYK, NOD2, LILRA5

GO-Term	Count	%	P-value	FDR	Genes
GO:0043020~NADPH oxidase complex	5	1	2.51E-04	1.06E-02	CYBA, NCF4, NCF2, RAC2, CYBB
GO:0038096~Fc-gamma receptor signaling pathway involved in phagocytosis	6	1	2.97E-04	3.37E-02	HCK, MYO1G, VAV1, PAK1, SYK, LYN

Supplementary Table 4 (partially) - Differentially expressed genes between macroscopically preserved and lesioned OA subchondral bone of patients with molecular endotype A OA.
The top 50 most significant differentially expressed genes between preserved and lesioned subchondral bone are shown here.

Ensembl ID	Gene name	Base mean	Log 2 fold change	Fold change	P-value	FDR
ENSG00000054938	CHRDL2	71.69	-3.88	0.07	2.98E-08	4.63E-04
ENSG00000102466	FGF14	19.50	-1.66	0.32	1.99E-07	7.73E-04
ENSG00000139718	SETD1B	260.38	-0.54	0.69	1.08E-07	7.73E-04
ENSG00000159307	SCUBE1	1579.37	-0.96	0.52	1.90E-07	7.73E-04
ENSG00000146830	GIGYF1	473.12	-0.31	0.80	3.88E-07	1.20E-03
ENSG00000252835	SCARNA21	607.24	0.43	1.35	4.69E-07	1.21E-03
ENSG00000153064	BANK1	90.61	-0.99	0.50	9.09E-07	2.01E-03
ENSG00000113594	LIFR	4351.68	0.38	1.30	1.61E-06	2.50E-03
ENSG00000134014	ELP3	389.12	0.26	1.20	1.56E-06	2.50E-03
ENSG00000167548	KMT2D	1048.61	-0.43	0.74	1.39E-06	2.50E-03
ENSG00000162998	FRZB	1002.99	-0.91	0.53	1.97E-06	2.77E-03
ENSG00000175573	C11orf68	132.68	-0.44	0.74	2.60E-06	3.36E-03
ENSG00000272333	KMT2B	289.54	-0.43	0.74	4.82E-06	5.75E-03
ENSG00000132359	RAP1GAP2	86.98	-0.65	0.64	6.46E-06	6.98E-03
ENSG00000167978	SRRM2	3172.15	-0.37	0.78	6.75E-06	6.98E-03
ENSG00000111676	ATN1	485.50	-0.47	0.72	9.92E-06	9.07E-03
ENSG00000270547	LINC01235	36.38	-1.95	0.26	9.94E-06	9.07E-03
ENSG00000196498	NCOR2	732.58	-0.52	0.70	1.33E-05	1.15E-02
ENSG00000129351	ILF3	903.85	-0.23	0.85	1.44E-05	1.18E-02
ENSG00000116698	SMG7	346.59	-0.31	0.81	1.67E-05	1.20E-02
ENSG00000122824	NUDT10	41.46	0.68	1.60	1.78E-05	1.20E-02
ENSG00000168488	ATXN2L	341.24	-0.38	0.77	1.77E-05	1.20E-02
ENSG00000179399	GPC5	29.20	-1.42	0.37	1.64E-05	1.20E-02
ENSG00000122756	CNTFR	51.10	-0.97	0.51	2.05E-05	1.31E-02
ENSG00000166925	TSC22D4	200.82	-0.44	0.74	2.18E-05	1.31E-02
ENSG00000182095	TNRC18	1076.27	-0.42	0.75	2.19E-05	1.31E-02
ENSG00000140443	IGF1R	653.60	-0.46	0.72	2.33E-05	1.34E-02
ENSG00000140416	TPM1	1974.72	0.42	1.33	2.75E-05	1.46E-02
ENSG00000177303	CASKIN2	363.75	-0.51	0.70	2.77E-05	1.46E-02
ENSG00000196104	SPOCK3	29.16	-2.50	0.18	2.83E-05	1.46E-02
ENSG00000187595	ZNF385C	17.57	-1.41	0.38	2.99E-05	1.49E-02

Ensembl ID	Gene name	Base mean	Log 2 fold change	Fold change	P-value	FDR
ENSG00000174469	CNTNAP2	99.27	1.38	2.60	3.13E-05	1.50E-02
ENSG00000204469	PRRC2A	1193.92	-0.41	0.75	3.20E-05	1.50E-02
ENSG00000104435	STMN2	76.11	4.61	24.40	3.37E-05	1.52E-02
ENSG00000110237	ARHGEF17	1030.01	-0.39	0.76	3.43E-05	1.52E-02
ENSG00000110046	ATG2A	216.72	-0.41	0.75	3.53E-05	1.52E-02
ENSG00000005339	CREBBP	1049.29	-0.38	0.77	4.36E-05	1.65E-02
ENSG00000074181	NOTCH3	3487.44	-0.62	0.65	4.47E-05	1.65E-02
ENSG00000115616	SLC9A2	17.72	1.41	2.66	4.27E-05	1.65E-02
ENSG00000116285	ERRFI1	749.87	0.62	1.54	4.39E-05	1.65E-02
ENSG00000175727	MLXIP	529.48	-0.30	0.81	4.19E-05	1.65E-02
ENSG00000184634	MED12	476.66	-0.31	0.80	4.23E-05	1.65E-02
ENSG00000187535	IFT140	157.77	-0.34	0.79	5.01E-05	1.81E-02
ENSG00000068697	LAPTM4A	1625.75	0.20	1.15	5.43E-05	1.88E-02
ENSG00000108175	ZMIZ1	1108.34	-0.44	0.74	5.93E-05	1.88E-02
ENSG00000108509	CAMTA2	206.76	-0.43	0.74	5.84E-05	1.88E-02
ENSG00000112584	FAM120B	348.12	-0.26	0.84	5.69E-05	1.88E-02
ENSG00000132024	CC2D1A	196.05	-0.33	0.79	5.70E-05	1.88E-02
ENSG00000148400	NOTCH1	964.62	-0.64	0.64	5.93E-05	1.88E-02
ENSG00000126461	SCAF1	211.18	-0.62	0.65	6.17E-05	1.91E-02

Supplementary Table 5 - Differentially expressed genes between macroscopically preserved and lesioned OA subchondral bone of patients with molecular endotype B OA.

Ensembl ID	Gene name	Base mean	Log 2 fold change	Fold change	P-value	FDR
ENSG00000108821	COL1A1	1.00E5	1.18	2.26	4.83E-08	6.52E-04
ENSG00000138755	CXCL9	123.45	-1.73	0.30	1.30E-07	8.56E-04
ENSG00000164694	FNDC1	574.56	1.07	2.10	1.90E-07	8.56E-04
ENSG00000156466	GDF6	64.10	4.06	16.69	6.71E-06	2.27E-02
ENSG00000006016	CRLF1	100.99	1.68	3.21	1.56E-05	2.77E-02
ENSG00000011028	AC080038.1	3290.14	0.81	1.75	1.64E-05	2.77E-02
ENSG00000107249	GLIS3	144.94	1.30	2.46	1.40E-05	2.77E-02
ENSG00000166741	NNMT	1482.53	0.77	1.71	1.53E-05	2.77E-02
ENSG00000100626	GALNT16	78.39	2.15	4.44	2.15E-05	3.23E-02
ENSG00000164692	COL1A2	1.09E5	0.91	1.88	2.56E-05	3.46E-02
ENSG00000211677	IGLC2	3393.08	0.97	1.96	3.71E-05	4.55E-02

Supplementary Table 6 (Partially) - Genes differentially expressed between molecular endotype A and B in both articular cartilage and subchondral bone.
With endotype A as reference, i.e. FC>1 means higher expressed in endotype B relative to endotype A. Top 50 most significant genes are shown here.

Ensembl ID	Gene name	Base mean cartilage	FDR cartilage	FD cartilage	Base mean bone	FDR bone	FD bone	Direction
ENSG00000105383	CD33	8.37	4.84E-16	11.08	112.33	6.27E-03	2.35	Similar
ENSG00000111679	PTPN6	49.75	1.04E-14	2.19	297.26	6.27E-03	3.87	Similar
ENSG00000204472	AIF1	33.67	6.91E-13	8.94	219.86	6.22E-03	2.53	Similar
ENSG00000120280	CXorf21	2.58	1.02E-11	12.05	48.52	4.23E-03	3.70	Similar
ENSG00000155629	PIK3AP1	22.27	7.14E-13	4.87	471.28	6.27E-03	2.43	Similar
ENSG00000151651	ADAM8	40.30	5.76E-13	4.58	137.70	7.59E-03	6.22	Similar
ENSG00000165025	SYK	26.65	1.70E-15	5.14	523.66	8.56E-03	3.13	Similar
ENSG00000204482	LST1	11.77	2.91E-10	7.78	145.88	1.60E-03	6.24	Similar
ENSG00000136167	LCP1	62.80	1.99E-11	5.79	1825.07	8.48E-03	4.37	Similar
ENSG00000158869	FCER1G	40.98	3.61E-14	8.16	255.04	1.12E-02	2.66	Similar
ENSG00000060558	GNA15	12.08	1.72E-11	7.55	97.03	8.56E-03	2.23	Similar
ENSG00000142347	MYO1F	33.38	3.52E-12	4.59	394.20	9.12E-03	4.43	Similar
ENSG00000169403	PTAFR	19.60	7.60E-12	7.37	145.17	9.28E-03	3.15	Similar
ENSG00000160883	HK3	16.58	2.71E-09	7.20	197.06	4.61E-03	12.26	Similar
ENSG00000100365	NCF4	15.45	1.85E-09	7.57	239.96	6.27E-03	4.12	Similar
ENSG00000089820	ARHGAP4	47.90	1.02E-15	4.04	315.67	1.84E-02	2.32	Similar
ENSG00000085514	PILRA	19.85	2.47E-09	3.13	68.17	6.39E-03	2.74	Similar
ENSG00000010671	BTK	8.88	3.08E-10	6.75	120.02	8.56E-03	3.81	Similar
ENSG00000132965	ALOX5AP	28.57	1.87E-08	6.07	197.85	5.78E-03	6.55	Similar

Ensembl ID	Gene name	Base mean cartilage	FDR cartilage	FD cartilage	Base mean bone	FDR bone	FD bone	Direction
ENSG00000086730	LAT2	17.34	3.81E-16	4.27	131.52	1.99E-02	3.02	Similar
ENSG00000126264	HCST	8.73	2.81E-10	3.42	91.28	8.91E-03	3.64	Similar
ENSG00000138756	BMP2K	74.66	3.50E-11	2.57	848.56	1.41E-02	1.94	Similar
ENSG00000163154	TNFAIP8L2	4.99	1.35E-08	6.12	48.58	6.27E-03	3.61	Similar
ENSG00000123338	NCKAP1L	40.87	4.38E-14	3.62	684.80	1.80E-02	2.28	Similar
ENSG00000169429	CXCL8	36.05	2.92E-08	10.74	47.25	5.83E-03	5.60	Similar
ENSG00000120549	KIAA1217	77.62	3.20E-11	4.93	460.17	1.58E-02	0.49	Opposite
ENSG00000170571	EMB	25.80	2.22E-08	6.00	559.88	6.28E-03	5.28	Similar
ENSG00000101336	HCK	26.39	3.93E-10	7.15	249.75	1.08E-02	3.26	Similar
ENSG00000100055	CYTH4	39.40	4.26E-15	8.65	377.78	2.11E-02	1.74	Similar
ENSG00000116701	NCF2	23.04	8.71E-07	3.52	397.12	3.49E-03	4.10	Similar
ENSG00000141968	VAV1	9.67	7.91E-12	6.29	174.37	1.92E-02	2.80	Similar
ENSG00000012779	ALOX5	21.79	5.99E-11	6.54	202.71	1.70E-02	5.38	Similar
ENSG00000198829	SUCNR1	2.58	9.85E-06	4.27	68.00	1.19E-04	6.10	Similar
ENSG00000186407	CD300E	8.23	8.49E-08	6.75	30.77	6.28E-03	4.01	Similar
ENSG00000163131	CTSS	127.88	2.42E-10	3.12	1064.78	1.48E-02	2.80	Similar
ENSG00000141480	ARRB2	73.74	2.30E-16	2.87	326.59	2.59E-02	2.25	Similar
ENSG00000075884	ARHGAP15	4.13	1.94E-10	10.16	127.68	1.63E-02	3.99	Similar
ENSG00000187116	LILRA5	1.98	5.11E-06	5.20	44.28	5.22E-03	10.04	Similar
ENSG00000003400	CASP10	9.96	8.34E-16	7.75	222.04	2.62E-02	1.72	Similar
ENSG00000140030	GPR65	2.80	5.29E-07	6.32	63.10	6.28E-03	2.76	Similar

Ensembl ID	Gene name	Base mean cartilage	FDR cartilage	FD cartilage	Base mean bone	FDR bone	FD bone	Direction
ENSG00000101916	TLR8	4.96	3.12E-05	4.82	87.89	3.88E-04	4.57	Similar
ENSG00000167851	CD300A	22.72	2.30E-12	3.40	94.05	2.52E-02	2.51	Similar
ENSG00000110934	BIN2	9.60	5.75E-09	5.40	192.87	1.30E-02	5.50	Similar
ENSG00000131042	LILRB2	14.83	3.32E-11	7.03	98.72	2.11E-02	2.83	Similar
ENSG00000081237	PTPRC	38.54	4.93E-09	5.10	964.12	1.44E-02	3.20	Similar
ENSG00000115232	ITGA4	10.82	5.55E-10	6.87	319.18	1.77E-02	4.62	Similar
ENSG00000128340	RAC2	26.03	1.85E-06	5.37	341.80	6.39E-03	6.85	Similar
ENSG00000123329	ARHGAP9	24.44	4.17E-05	2.96	160.76	3.70E-03	5.00	Similar
ENSG00000115956	PLEK	35.29	3.46E-08	4.23	613.11	1.12E-02	3.73	Similar
ENSG00000244482	LILRA6	8.79	2.15E-08	5.31	36.32	1.37E-02	4.14	Similar

Supplementary Table 7 - Gene enrichment on genes differentially expressed between endotype A and B in both articular cartilage and subchondral bone, with similar directions of effect.

GO-Term	Count	%	P-value	FDR	Genes
GO:0005886~plasma membrane	91	52	4.59E-16	1.06E-13	CD38, BTK, PLAUR, TYROBP, ACPP, WAS, GNA15, DAPP1, STXBP2, PTPRC, PILRA, LAT2, CYTH4, GRAP2, NCF4, CSF2RB, RASSF2, HCK, TLR8, CORO1A, LILRB1, CD33, PIK3CG, ZBTB16, BIN2, CLEC4A, TREML2, ITGA4, PLEK, NCF2, LRMP, VAMP8, ADCY7, CCRL2, ARL4A, CNTFR, NCKAP1L, HCST, CFP, RAC2, LRRC4, ATP8B3, LILRB2, CD180, DOCK2, PLXNC1, LCP1, MYO1G, GYPC, CASP1, GPR84, GPR65, ARRB2, VAV1, MYO1F, SIGLEC10, SLC2A5, EFHD2, CD53, RGS18, ADAM8, ARL11, PIK3AP1, CD1C, FCER1G, JAML, CD200R1, SYK, CYBB, MELK, NOD2, SNX20, CD300A, PTAFR, EMB, FPR1, RGS19, CD300LB, CD300LF, CD300E, LILRA5, SIRPB2, C5AR1, SLC28A3, SUCNR1, LST1, LILRB3, IGLV1-40, IGLV3-21, GPSM3, LILRA6
GO:0006955~immune response	22	13	8.09E-10	1.05E-06	WAS, LCP2, OSM, TLR8, PIK3CG, CLEC4A, CCRL2, IL1B, CFP, LILRB2, GPR65, IGSF6, VAV1, CD1C, CTSS, PTAFR, CXCL8, C5AR1, LST1, IGLV1-40, IGLV3-21, GPSM3
GO:0070821~tertiary granule membrane	10	6	8.78E-08	1.01E-05	CD33, VAMP8, LILRB2, GPR84, CD53, ADAM8, FCER1G, CYBB, CD300A, PTAFR
GO:0030593~neutrophil chemotaxis	9	5	3.04E-07	1.97E-04	PIK3CG, NCKAP1L, IL1B, VAV1, FCER1G, JAML, SYK, CXCL8, C5AR1
GO:0032755~positive regulation of interleukin-6 production	10	6	7.86E-07	3.39E-04	BTK, TYROBP, TLR8, IL1B, LILRB2, SYK, NOD2, PTAFR, LILRA5, AIF1
GO:0032396~inhibitory MHC class I receptor activity	5	3	1.16E-06	4.03E-04	LILRB1, LILRB2, LILRA5, LILRB3, LILRA6
GO:0002250~adaptive immune response	14	8	1.99E-06	6.45E-04	BTK, LAT2, LILRB1, PIK3CG, CLEC4A, LILRB2, SIGLEC10, CD1C, CTSS, SYK, LILRB3, IGLV1-40, IGLV3-21, LILRA6
GO:0030667~secretory granule membrane	9	5	1.27E-05	7.69E-04	CD38, TYROBP, PTPRC, VAMP8, NCKAP1L, PTAFR, FPR1, C5AR1, LILRB3
GO:0001891~phagocytic cup	6	3	1.33E-05	7.69E-04	CORO1A, BIN2, LCP1, MYO1G, ARHGAP25, AIF1

GO-Term	Count	%	P-value	FDR	Genes
GO:0032731~positive regulation of interleukin-1 beta production	8	5	2.98E-06	7.71E-04	TYROBP, NLRC4, TLR8, CASP1, GBP5, MNDA, NOD2, LILRA5
GO:0006954~inflammatory response	16	9	6.49E-06	1.40E-03	LYZ, NLRC4, HCK, TLR8, PIK3CG, CCRL2, IL1B, CD180, ADAM8, GBP5, CYBB, PTAFR, CXCL8, FPR1, C5AR1, AIF1
GO:0019221~cytokine-mediated signaling pathway	10	6	8.75E-06	1.62E-03	CSF2RB, HCK, LILRB1, PTPN6, CNTFR, IL1B, LILRB2, LILRA5, LILRB3, LILRA6
GO:0045087~innate immune response	18	10	1.31E-05	2.12E-03	BTK, NLRC4, HCK, TLR8, CORO1A, PIK3CG, CLEC4A, NCF2, CXorf21, CD180, SIGLEC10, FCER1G, TNFAIP8L2, SYK, CYBB, NOD2, APOBEC3B, LILRA5
GO:0006935~chemotaxis	9	5	1.66E-05	2.15E-03	PLAUR, CCRL2, NCKAP1L, RAC2, DOCK2, PTAFR, CXCL8, FPR1, C5AR1
GO:0032760~positive regulation of tumor necrosis factor production	9	5	1.66E-05	2.15E-03	BTK, TYROBP, PTPRC, SASH3, SYK, CYBB, NOD2, PTAFR, LILRA5
GO:0005887~integral component of plasma membrane	28	16	4.94E-05	2.28E-03	PLAUR, TYROBP, PTPRC, CSF2RB, CD33, CLEC4A, LRMP, ADCY7, CCRL2, NCKAP1L, LILRB2, PLXNC1, GYPC, GPR84, GPR65, IGSF6, SLC2A5, CD53, ADAM8, CD1C, FCER1G, CYBB, PTAFR, EMB, EVI2B, C5AR1, SLC28A3, LILRB3
GO:0002376~immune system process	7	4	2.18E-05	2.35E-03	NLRC4, LRMP, NOD2, CD300A, CD300LB, CD300LF, CD300E
GO:0007165~signal transduction	28	16	2.18E-05	2.35E-03	CD38, PLAUR, TYROBP, DAPP1, ARHGAP15, PILRA, ARHGAP4, GRAP2, CSF2RB, RASSF2, LILRB1, CD33, STMN1, CNTFR, ARHGAP9, IL1B, RAC2, GMFG, LILRB2, CASP1, ARRB2, CD53, ARHGAP25, CD200R1, CXCL8, FPR1, ARHGAP30, C5AR1
GO:0035579~specific granule membrane	8	5	7.98E-05	3.07E-03	PLAUR, CD33, VAMP8, GPR84, SLC2A5, CD53, ADAM8, CYBB
GO:0042102~positive regulation of T cell proliferation	7	4	3.44E-05	3.43E-03	PTPRC, CORO1A, SASH3, NCKAP1L, IL1B, LILRB2, AIF1
GO:0032695~negative regulation of interleukin-12 production	5	3	4.90E-05	4.53E-03	TLR8, LILRB1, ARRB2, NOD2, LILRA5

GO-Term	Count	%	P-value	FDR	Genes
GO:0050853~B cell receptor signaling pathway	8	5	1.09E-04	9.38E-03	CD38, BTK, PTPRC, LAT2, PTPN6, NCKAP1L, MNDA, SYK
GO:0002675~positive regulation of acute inflammatory response	4	2	1.79E-04	1.44E-02	OSM, PIK3CG, ALOX5AP, ADAM8
GO:0101003~ficolin-1-rich granule membrane	6	3	4.41E-04	1.45E-02	NCKAP1L, LILRB2, ADAM8, FCER1G, CD300A, FPR1
GO:0043020~NADPH oxidase complex	4	2	5.15E-04	1.49E-02	NCF4, NCF2, RAC2, CYBB
GO:0045089~positive regulation of innate immune response	5	3	2.22E-04	1.69E-02	TLR8, CXorf21, ADAM8, GBP5, NOD2
GO:0035580~specific granule lumen	6	3	6.60E-04	1.69E-02	LYZ, PTPN6, QPCT, CFP, DOCK2, HPSE
GO:0050727~regulation of inflammatory response	7	4	2.82E-04	2.03E-02	ALOX5, HCK, CASP1, PIK3AP1, NOD2, TMSB4X, GPSM3
GO:0009986~cell surface	16	9	1.01E-03	2.33E-02	CD38, PLAUR, TYROBP, PTPRC, CD33, TREML2, ITGA4, HCST, LILRB2, CD53, ADAM8, FCER1G, CD200R1, NOD2, LILRA5, C5AR1
GO:0005576~extracellular region	30	17	1.24E-03	2.54E-02	PLAUR, ALOX5, STXBP2, LYZ, OSM, LILRB1, BIN2, ACRBP, PTPN6, QPCT, PLEK, GLIPR2, ARHGAP9, IL1B, CFP, GMFG, DOCK2, AOAH, CASP1, SIGLEC10, HK3, CTSS, MNDA, CD200R1, CXCL8, HPSE, LILRA5, TMSB4X, IGLV1-40, IGLV3-21
GO:0032010~phagolysosome	3	2	1.32E-03	2.54E-02	NCF4, NCF2, ADAM8
GO:0032720~negative regulation of tumor necrosis factor production	6	3	4.51E-04	3.07E-02	LILRB1, CD33, PTPN6, CLEC4A, ARRB2, NOD2
GO:0009897~external side of plasma membrane	12	7	1.83E-03	3.25E-02	PTPRC, CSF2RB, TLR8, LILRB1, CD33, CLEC4A, ITGA4, CCRL2, CNTFR, CD1C, FCER1G, CD200R1
GO:0050729~positive regulation of inflammatory response	7	4	7.35E-04	4.35E-02	NLRC4, OSM, IL1B, CASP1, LILRA5, SUCNR1, GPSM3

GO-Term	Count	%	P-value	FDR	Genes
GO:0035556~intracellular signal transduction	14	8	7.37E-04	4.35E-02	BTK, TYROBP, LCP2, LAT2, PTPN6, ECT2, STMN1, ADCY7, PLCL2, CD200R1, SYK, MELK, NOD2, CXCL8
GO:0050790~regulation of catalytic activity	13	7	7.43E-04	4.35E-02	BTK, WAS, ARHGAP4, CYTH4, NCF4, NCF2, RAC2, ALOX5AP, DOCK2, BMP2K, RGS18, ARHGAP30, GPSM3
GO:0045730~respiratory burst	4	2	7.92E-04	4.35E-02	NCF4, NCF2, RAC2, CYBB
GO:0038156~interleukin-3-mediated signaling pathway	3	2	8.07E-04	4.35E-02	CSF2RB, FCER1G, SYK
GO:0030889~negative regulation of B cell proliferation	4	2	9.53E-04	4.55E-02	BTK, TYROBP, MNDA, CD300A
GO:0030890~positive regulation of B cell proliferation	5	3	9.85E-04	4.55E-02	CD38, BTK, PTPRC, SASH3, NCKAP1L
GO:0042098~T cell proliferation	5	3	9.85E-04	4.55E-02	PTPRC, CORO1A, PIK3CG, PTPN6, SASH3
GO:0006968~cellular defense response	5	3	9.85E-04	4.55E-02	TYROBP, NCF2, LILRB2, MNDA, C5AR1
GO:1904813~ficolin-1-rich granule lumen	7	4	2.93E-03	4.83E-02	ALOX5, BIN2, QPCT, GMFG, HK3, CTSS, MNDA
GO:0005884~actin filament	6	3	3.14E-03	4.83E-02	WAS, HCK, CORO1A, RAC2, LCP1, AIF1
GO:1904724~tertiary granule lumen	5	3	3.35E-03	4.83E-02	LYZ, PTPN6, QPCT, CFP, CTSS
GO:0031663~lipopolysaccharide-mediated signaling pathway	5	3	1.09E-03	4.85E-02	SPI1, HCK, IL1B, CD180, PTAFR

Supplementary Table 8 - Genes differentially expressed between preserved and lesioned OA articular cartilage and subchondral bone exclusively for molecular endotype A.

Ensembl ID	Gene name	Base mean cartilage	FDR cartilage	FD cartilage	Base mean bone	FDR bone	FD bone	Direction
ENSG00000008441	NFIX	1462.89	4.66E-02	0.74	690.67	1.96E-02	0.69	Similar
ENSG00000125430	HS3ST3B1	81.50	2.71E-02	0.68	24.82	2.47E-02	0.49	Similar
ENSG00000129351	ILF3	805.88	2.57E-02	0.92	903.85	1.18E-02	0.85	Similar